Modulation of Electroosmotic Flow by Neutral Polymers

Rui Qiao* and Ping He

Department of Mechanical Engineering, Clemson University, Clemson, South Carolina 29634

Received October 16, 2006. In Final Form: February 2, 2007

Polymer coating is widely used to modulate the fluid flow in micro- and nanometer pores and flows that are sensitive to surface properties such as electroosmotic flow. Here we report on the dissipative particle dynamics simulations of the modulation of electroosmotic flow by neutral polymers. In these coarse-grained simulations, fluid and polymers are resolved at a scale comparable to polymer size and the two-way coupling between polymer conformation and fluid flow are explicitly accounted for. The simulations indicate that, in the parameter space explored, the screening of electroosmotic flow by polymers decreases nonlinearly as the external electric field increases. Such an observation is understood by analyzing the surface coverage by polymers, height and orientation of the grafted polymers, and the two different modes of flow screening by polymer segments as a function of the external electric field. Understanding the effects and interplay of these physical processes is crucial for the rational design of polymer coating for flow control in microfluidic and nanofluidic systems.

I. Introduction

Polymer coating is widely used to regulate fluid transport in micro- and nanometer pores and fluid transport sensitive to surface properties. For example, solvent permeability through porous membrane can be controlled by grafting polymers on the membrane surfaces[1−4] and electroosmotic flow near charged surfaces can be quenched by grafting or physically adsorbing polymers on the surfaces.[5−9] Polymer coating can modulate fluid transport by several mechanisms such as by changing the effective size of fluidic channels, by rendering viscous drag to the fluids, and by modifying the phyicochemical properties of the host surfaces. Understanding the effects and possible interplay between these mechanisms is of great interest both from a fundamental science perspective and engineering perspective.

Here we study the modulation of electroosmotic flow by polymer grafting. Electroosmotic flow is widely encountered in micro- and nanofluidic systems.[10] When an ionic solution is in contact with a charged surface, an electrical double layer with a net charge develops near the surface. If an external electrical field is applied in the direction tangential to the surface, the fluid will be dragged by the moving ions in the electrical double layer and an electroosmotic flow is induced. In many applications, e.g., bio-molecule separations, polymer coating is used to minimize the electroosmotic flow and to reduce the analyte adsorption on channel surfaces.[5−9] Though a large amount of empirical knowledge has been accumulated on the performance of different polymer coatings, a thorough understanding of its flow control mechanisms is still lacking. The key challenges in understanding such modulation are the two-way coupling between polymer deformation and fluid transport and the scale separation between molecular lengths and polymer size. So far, only a handful of theoretical studies have been reported.[11−14] Harden et al. reported the first analytical study of electroosmotic flow modulation by polymer using a scaling analysis,[11] and both very low grafting density scenario (the mushroom regime) and high grafting density scenario (the brush regime) were studied. While their study provided significant insight into the coupling between polymer deformation and flow modulation, it is based solely on scaling argument and its applicability in the regime intermediate between different regimes of the parameter space (e.g., for grafting density between mushroom and brush regimes) is not clear. Most recently, Tessier and Slater studied the effects of polymer chain length and coating density on electroosmotic flow systematically by using coarse-grained molecular dynamics simulations,[13] and we analyzed the effects of polymer coating on the ion distribution (and thus the electroosmotic flow) in electrical double layers by modeling the water and ions explicitly using full scale molecular dynamics simulations.[14] While these simulations improved our understanding of the mechanisms of electroosmotic flow control by polymer coating, they can only probe a small parameter space due to their high computational cost, and many important issues, e.g., field strength dependence of the flow modulation as predicted in ref 11, cannot be studied effectively.

Dissipative particle dynamics (DPD) is a mesoscopic particle method developed for the simulation of complex fluids.[15,16] Unlike the particles in molecular dynamics model, particles in a DPD model (called "beads") represent a packet of fluid atoms moving collectively. By neglecting the atomistic details of fluids, DPD simulations can reach time and length scales orders of magnitude larger than the classical molecular dynamics simulations.[17] Though the original DPD model is heuristic in nature, theoretical foundations of the DPD model have been established recently.

* To whom correspondence should be addressed. Email: rqiao@ces.clemson.edu. URL: http://www.clemson.edu/ rqiao.

(1) Ito, Y.; Park, Y. S.; Imanishi, Y. *Langmuir* **2000**, *16*, 5376.
(2) Castro, R. P.; Monbouquette, H. G.; Cohen, Y. *J. Membr. Sci.* **2000**, **179**, 207.
(3) Hautojarvi, J.; Kontturi, K.; Nasman, J. H.; Svarfvar, B. L.; Viinikka, P.; Vuoristo, M. *Ind. Eng. Chem. Res.* **1996**, *35*, 450.
(4) Peng, T.; Cheng, Y. L. *J. Appl. Polym. Sci.* **1998**, *70*, 2133.
(5) Hjerten, S. *J. Chromatogr.* **1985**, *347*, 191.
(6) Gao, Q. F.; Yeung, E. S. *Anal. Chem.* **1998**, *70*, 1382.
(7) Doherty, E. A. S.; Berglund, K. D.; Buchholz, B. A.; Kourkine, I. V.; Przybycien, T. M.; Tilton, R. D.; Barron, A. E. *Electrophoresis* **2002**, *23*, 2766.
(8) Cretich, M.; Chiari, M.; Pirri, G.; Crippa, A. *Electrophoresis* **2005**, *26*, 1913.
(9) Catai, J. R.; Tervahauta, H. A.; de Jong, G. J.; Somsen, G. W. *J. Chromatogr. A* **2005**, *1083*, 185.
(10) Vilkner, T.; Janasek, D.; Manz, A. *Anal. Chem.* **2004**, *76*, 3373.
(11) Harden, J. L.; Long, D.; Ajdari, A. *Langmuir* **2001**, *17*, 705.
(12) Tessier, F.; Slater, G. W. *Macromolecules* **2005**, *38*, 6752.
(13) Tessier, F.; Slater, G. W. *Macromolecules* **2006**, *39*, 1250.
(14) Qiao, R. *Langmuir* **2006**, *22*, 7096.
(15) Hoogerbrugge, P. J.; Koelman, J. M. V. A. *Euro. Phys. Lett.* **1992**, *19*, 155.
(16) Groot, R. D.; Warren, P. B. *J. Chem. Phys.* **1997**, *107*, 4423.
(17) Symeonidis, V.; Karniadakis, G. E.; Caswell, B. *Comput. Sci. Eng.* **2005**, *7*, 39.

10.1021/la063042v CCC: $37.00
Published on Web 04/14/2007 PAGE EST: 6.4

Thermal fluctuations and thermostat are directly built in the DPD model,[16,18] and the model has been shown to produce correct hydrodynamic behavior, i.e., the Navier−Stokes equations emerges at a long-wavelength limit and a unique viscosity can be defined.[19] DPD model has been used successfully to investigate the structure and rheology of colloidal and polymer suspensions,[20,21] as well as the relaxation dynamics of DNA in bulk solutions.[22] DPD simulations of the response of polymer conformation to steady and oscillatory shear flow were reported by Wijmans and Smit,[23] and most recently, the control of pressure driven flow in nanofluidic channels by polymer brushes was investigated by Huang et al. using the same method.[24]

In this paper, we investigate the screening of electroosmotic flow by polymer as a function of the external electrical field by using DPD simulations. The rest of the paper is organized as follows. Section II describes the simulation methods and system, and Section III presents the simulation results and discussion. Finally, conclusions are presented in Section IV.

II. Simulation Methods and System

A. Dissipative Particle Dynamics Method. DPD is a stochastic simulation method. DPD particles (beads) interact with each other via three types of forces: a repulsive conservative force, a dissipative force that reduces the velocity difference between particles, and a random force acting along the line connecting the particles. The equations of motion of a DPD system are[16]

$$d\mathbf{r}_i = \boldsymbol{v}_i dt \tag{1}$$

$$m d\boldsymbol{v}_i = \boldsymbol{F}_i^C dt + \boldsymbol{F}_i^D dt + \boldsymbol{F}_i^R \sqrt{dt} \tag{2}$$

where m, $\mathbf{r}_i$, and v_i are the mass, position, and velocity of bead i, respectively. In the present simulations, m_i is taken to be same for all beads. dt is the time step size. $\boldsymbol{F}_i^C$, $\boldsymbol{F}_i^D$, and $\boldsymbol{F}_i^R$ are the conservative, dissipative, and random force acting on particle i, and they are given by

$$\boldsymbol{F}_i^C = \sum_{j \neq i} a_{ij} w(r_{ij}/r_c) \boldsymbol{e}_{ij} \tag{3}$$

$$\boldsymbol{F}_i^D = \sum_{j \neq i} -\gamma_{ij} w^2(r_{ij}/r_c)(\boldsymbol{e}_{ij} \cdot \boldsymbol{v}_{ij}) e_{ij} \tag{4}$$

$$\boldsymbol{F}_i^R = \sigma_{ij} w(r_{ij}/r_c) \theta_{ij} \boldsymbol{e}_{ij} \tag{5}$$

where a_{ij} is the conservative force coefficient and $r_{ij} = |\boldsymbol{r}_{ij}| = |\boldsymbol{r}_i - \boldsymbol{r}_j|$. r_c is the cutoff length for the conservative, dissipative, and random interactions between particle i and j. $\boldsymbol{e}_{ij} = \boldsymbol{r}_{ij}/r_{ij}$ is the unit vector pointing from particle i to particle j and $\boldsymbol{v}_{ij} = \boldsymbol{v}_i - \boldsymbol{v}_j$ is the relative velocity between particles i and j. θ_{ij} are symmetric random variables with zero mean and unit variance. w is a weighting function. In the present simulations, it takes the form of

$$w(r_{ij}) = \begin{cases} 1 - r_{ij}/r_c & \text{for } r_{ij} < r_c \\ 0 & \text{for } r_{ij} \geq r_c \end{cases} \tag{6}$$

Variables γ_{ij} and σ_{ij} determine the strength of the dissipative and random force, and are related to each other by the fluctuation−dissipation theorem

$$\sigma_{ij}^2 = 2k_B T \gamma_{ij} \tag{7}$$

where k_B and T are the Boltzmann constant and temperature, respectively. Variables in DPD models are presented in reduced units, where the mass, length, and energy are measured by m, r_c, k_BT, respectively. Velocity is measured by $[v] = \sqrt{3k_BT/m}$ and time is measured by $[t] = r_c/[v]$.[22]

B. DPD Simulation of Electroosmotic Flow Modulation by Polymer. Figure 1A shows a schematic of the simulation system. The system consists of a slab of fluid beads enclosed by two channel walls, and each wall is grafted with four polymers. The lateral dimensions of the channel are 10 × 10, and the channel width, W, is 16. Flow is in the x direction and periodic boundary conditions are used in the x and y directions.

Fluids are modeled as single DPD beads with a number density of 4.0. Each polymer is modeled as a 16-bead finitely extensible nonlinear elastic (FENE) chain. Such a polymer model has been shown to exhibit realistic volume exclusion effects recently.[22,25] In the simulations, polymer beads experience the standard DPD forces, as shown in eqs 3−5. In addition, they are subject to intrapolymer interactions. In an FENE chain, the intrapolymer potential between two neighbor beads i and $i + 1$ is given by

$$U_{\mathrm{FENE}} = -\frac{k}{2} r_{\max}^2 \log[1 - |r_i - r_{i+1}|^2/r_{\max}^2] \tag{8}$$

where k is a spring constant and $r_{\max}$ is maximum bond extension between bead i and $i + 1$.

The implementation of channel walls is a nontrivial problem in DPD simulations. The two key requirements, namely, impermeability to fluids and producing accurate boundary condition for fluids velocity, are difficult to achieve by using the methods adopted in molecular dynamics simulations. Due to the soft-repulsive nature of the conservative interactions between beads, fluid beads can penetrate the channel wall and no-slip boundary condition cannot be reproduced unless a very large number of wall beads are used. The high number density of wall beads, however, will incur significant and artificial density oscillation near the surface.[26] Here we adopt the methods proposed by Duong-Hong et al.[27] to implement impermeable channel walls with no-slip boundary condition. As shown in Figure 1B, each channel wall consists of two components: an imaginary surface $A - A'$ and two layers of wall atoms (arranged in square lattice) close to the imaginary surface. The conservative interaction between the fluid beads and wall beads are tuned by following the method proposed by Pivkin and Karniadakis[28] to minimize the fluids density oscillation near the wall. To enforce the no-slip boundary condition and wall impermeability, a bead i that crosses the imaginary surface $A - A'$ during a time step is "kicked back" into the channel,[27,28] i.e.,

$$\boldsymbol{v}_i' = -\boldsymbol{v}_i \tag{9}$$

$$\boldsymbol{r}_i' = \boldsymbol{r}_i + 2d_r \boldsymbol{n}_w \tag{10}$$

where $\boldsymbol{v}_i$ and $\boldsymbol{r}_i$ are the velocity and position of bead i at the end of time step should no action is taken, and $\boldsymbol{v}_i'$ and $\boldsymbol{r}_i'$ are the velocity and position of the bead after the "kick-back" is enforced. d_r is the distance from the bead to the imaginary surface, and $\boldsymbol{n}_w$ is the normal vector on the wall directing into the channel.

An explicit simulation of electroosmotic flow requires that the electrical double layer to be resolved and the fluids, ions, and polymers to be modeled at the atomistic level, as have been done in earlier molecular dynamics simulations.[13,14] Adopting such an approach in a DPD simulation essentially means that the coarse-graining level is comparable to the molecular scale. This necessitates a large number

(18) Espanol, P.; Warren, P. *Europhys. Lett.* **1995**, *30*, 191.
(19) Marsh, C.; Backx, G.; Ernst, M. H. *Phys. Rev. E* **1997**, *56*, 1676.
(20) Martys, N. S. *J. Rheol.* **2005**, *49*, 401.
(21) Spenley, N. A. *Europhys. Lett.* **2000**, *49*, 534.
(22) Symeonidis, V.; Karniadakis, G. E.; Caswell, B. *Phys. Rev. Lett.* **2005**, *95*, 076001.
(23) Wijmans, C. M.; Smit, B. *Macromolecules* **2002**, *35*, 7138.
(24) Huang, J. H.; Wang, Y. M.; Laradji, M. *Macromolecules* **2006**, *39*, 5546.
(25) Symeonidis, V.; Karniadakis, G. E. *J. Comput. Phys.* **2006**, *218*, 82.
(26) Willemsen, S. M.; Hoefsloot, H. C. J.; Iedema, P. D. *Intl. J. Modern Phys.* **2000**, *11*, 881.
(27) Duong-Hong, D.; Phan-Thien, N.; Fan, X. J. *Comput. Mech.* **2004**, *35*, 24.
(28) Pivkin, I. V.; Karniadakis, G. E. *J. Comput. Phys.* **2005**, *207*, 114.

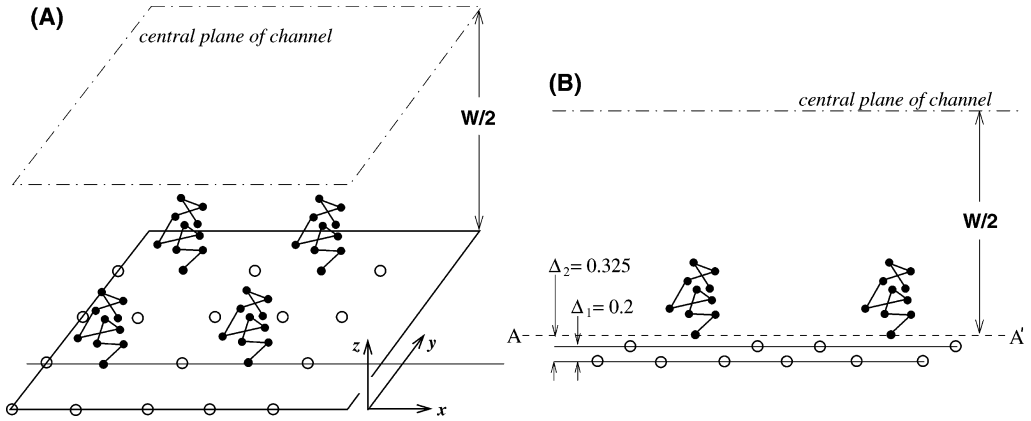

Figure 1. (A) Schematic of the simulation system. Only the lower half of the channel is shown because of the symmetry, and fluid beads are not shown for clarity. Circles denote the wall beads, and filled circles denote the polymer beads. (B) Side view of the simulation system and structure of the channel wall.

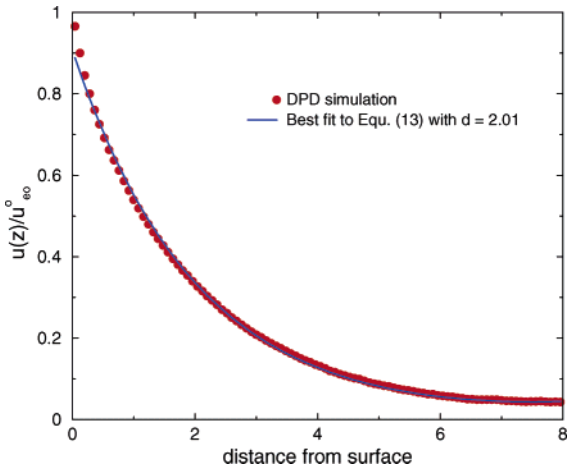

Figure 2. Comparison of the velocity profile near channel surface grafted with four vertically oriented polymers as obtained from DPD simulation and its best fit to eq 13.

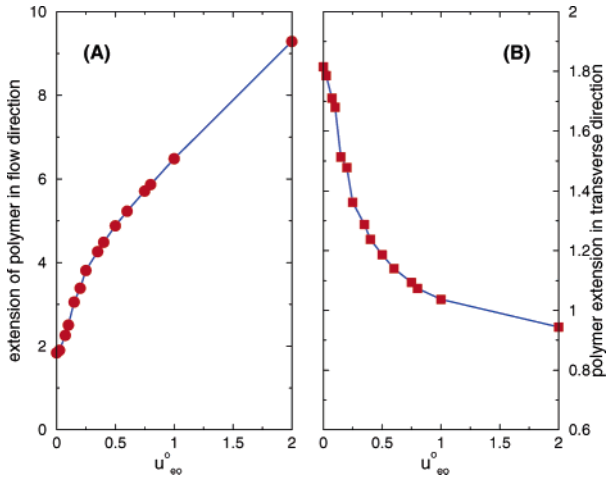

Figure 3. Scaling of the stretching of polymer in the flow direction (A) and transverse direction of flow (B) as the unscreened electroosmotic velocity u°_{eo} (or equivalently, the external electrical field) increases. The solid lines are guides for the eyes.

of beads to be used when long-chain polymers are present. To circumvent this difficulty, we note that most often the electrical double layer is not resolved in the analytical studies and computational fluid dynamics simulations of electroosmotic flow.[11,29,30] Instead, the surface is often modeled as a slip-plane with a slip velocity

$$u_{eo} = -\zeta \epsilon E_{ext}/\eta \tag{11}$$

where ζ is the ζ-potential of the surface, ϵ is the permittivity of fluid, E_{ext} is the external electric field, and η is the dynamic viscosity of fluids. Such an approach is accurate if the thickness of electrical double layer (as characterized by the Debye length) is much smaller compared to the channel width and characteristic dimension of polymer (e.g., radius of gyration).[11] Since the Debye length ranges typically from a few angstroms to tens of nanometers, such a requirement is usually satisfied for microfluidic channels coated with long-chain polymers. Therefore, we implement the electroosmotic flow in our DPD model as follows. If a fluid bead crosses the imaginary surface $A - A'$ shown in Figure 1B, it is bounced back as in eq 10 and its velocity is changed to

$$\boldsymbol{v}_i' = -\boldsymbol{v}_i + 2u_{eo}\boldsymbol{e}_x \tag{12}$$

where $\boldsymbol{e}_x$ is the unit vector in the flow direction (x direction in the present simulations). Such an implementation ensures that the average velocity of fluid beads adjacent to a uncovered channel wall is u_{eo}.

Table 1. Parameters Used in the Dissipative Particle Dynamics Simulations[a]

param	value	eq	param	value	eq	param	value	eq
a_{f-f}	18.75	3	a_{f-w}	6.70	3	r_{max}	1.50	8
a_{f-p}	18.75	3	a_{p-w}	6.70	3	σ	3.00	7
a_{p-p}	18.75	3	k	30.0	3	T	1.00	7

[a] f, p, and w denote the fluid, polymer, and wall beads, respectively.

For the polymer beads, the "kickback" scheme described by eq 9 is used. In this paper, we study the different behavior of electroosmotic flow near polymer coated surfaces. In all the simulations, the physicochemical properties of uncoated surface and fluids (e.g., ζ potential and fluid viscosity) are the same, and the different unscreened electroosmotic velocities are obtained by varying the external electrical field.

Equations 1 and 2 were integrated using the modified Verlet algorithm[16] with a time step of 0.01. The number of DPD beads is 7424 for each of the case studied here. For each simulation, starting from a random configuration, an equilibrium run of 200 000 steps was first performed so that polymers and fluids relax to their equilibrium configuration. This was followed by a nonequilibrium run (with electroosmotic flow implemented) of 100 000 steps for the system to reach a steady state. After that, a production run of 400 000 to 1 000 000 steps was performed. Table 1 summarizes the simulation parameters used in the simulations presented in Section III.

(29) Chen, C. H.; Lin, H.; Lele, S. K.; Santiago, J. G. *J. Fluid Mech.* **2005**, *524*, 263.
(30) Xuan, X. C.; Li, D. Q. *J. Colloid Interface Sci.* **2005**, *289*, 291.

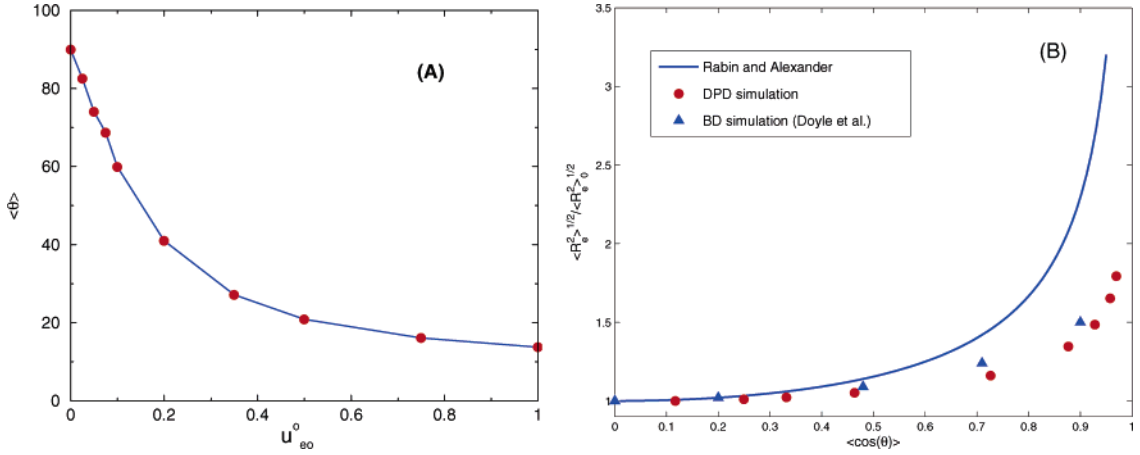

Figure 4. (A) Variation of the orientation of polymer in the flow direction as a function of the electroosmotic velocity u°_{eo}. (B) Comparison of the chain stretch and inclination as obtained from analytical theory,[31] DPD simulations and Brownian Dynamics simulations.[32] In the Brownian simulation, the polymer chain has 20 beads.

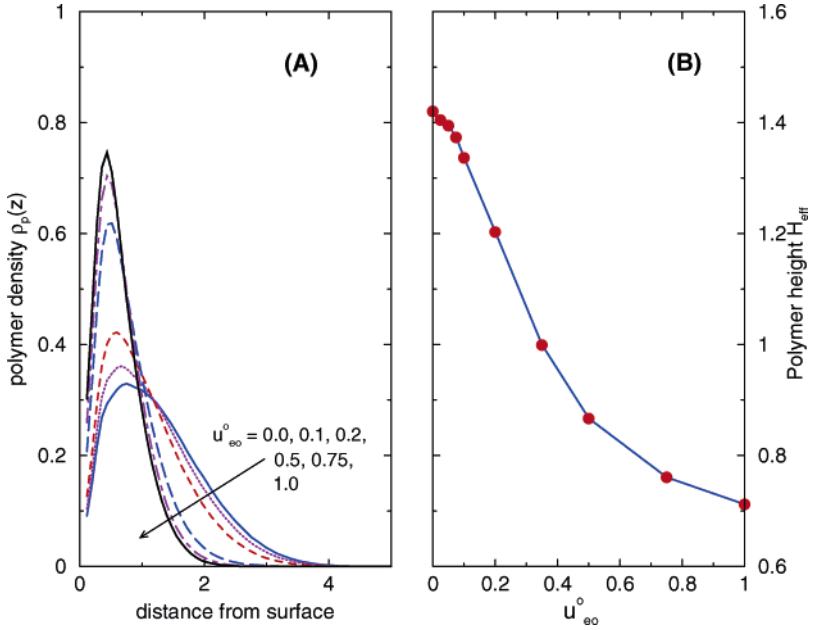

Figure 5. Variation of the polymer density near surface (A) and effective polymer height H_{eff} (B) at different electroosmotic velocities.

III. Results and Discussion

A. Code Validation. The DPD code developed has been tested extensively. The pressure-driven flow in slit channels studied in earlier publications[27,28] was simulated under the same condition as reported. The density oscillation near the channel wall is very small (<5% of the bulk density), and the no-slip boundary condition was observed. The velocity profile obtained is in excellent agreement with the earlier reports. Scaling of radius of gyration, R_g, of a single polymer in good solvent was also studied, and the scaling exponent, ν, as in $R_g \propto (N-1)^{\nu}$ (N is the number of beads in the polymer), was found to be 0.61. This result confirms that the Flory's exponent is recovered in our simulation, and the result is also in good agreement with earlier DPD simulations.[22,24]

To investigate the effectiveness of the method proposed in Section II.B for modeling electroosmotic flow, we simulated electroosmotic flow in channels without polymer grafting. In these simulations, the channel surface is "covered" (i.e., fluid bead colliding with it is bounced back following eq 9 instead of eq 12) to different extents (each characterized by a coverage ratio, α, defined as the ratio between area of wall with boundary condition given by eq 9 to the total wall area), and the velocity in the channel was analyzed. The average velocity at the channel center, u_c, is found to agree with the analytical prediction $u_c = u^{\circ}_{eo}(1-\alpha)$ almost perfectly, indicating that the proposed method can model electroosmotic flow effectively.

To further investigate whether the screening of electroosmotic flow by polymer can be modeled with good accuracy, we orient each of the eight polymers vertically and freeze them during the simulation. The spacing between neighboring polymer beads is set to 0.5, giving a total height, H, of 7.5 for each polymer. The electroosmotic velocity u°_{eo} at the channel surface is set to 1.0. The velocity profile near channel surface has an analytical solution[11]

$$u(z) = u^{\circ}_{eo}\frac{\cosh((H-z)/d)}{\cosh(H/d)} \tag{13}$$

where d is the effective spacing between polymers. Figure 2shows the velocity obtained from DPD simulation and the best fit to eq 13 using d as a fitting parameter. While it is difficult to fit the DPD results to eq 13 in the entire domain, the DPD results

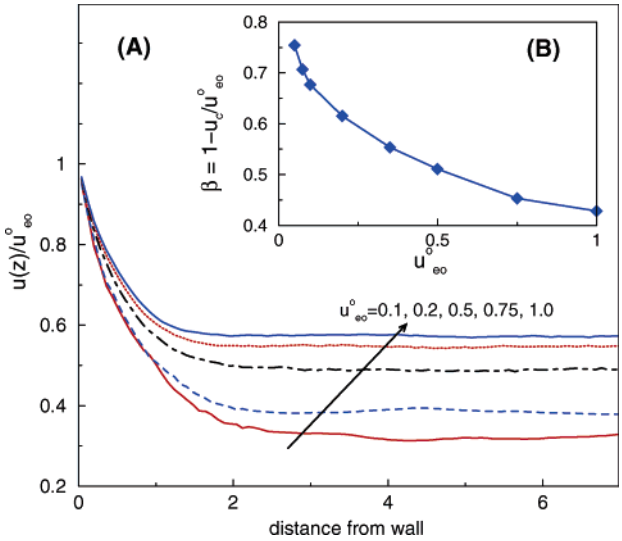

Figure 6. (A) Velocity profiles near surface for various unscreened electroosmotic velocities u_{eo}°. (B) Scaling of electroosmotic velocity screening factor, β, as a function of u_{eo}°.

can be fitted to eq 13 very well in the region $z > 0.3$. The discrepancy in the region $z < 0.3$ may be caused by the fact that grafted polymers cover some parts of the channel surface, which certainly affects the velocity profile but is not accounted for in the analytical solution.

B. Conformation of Polymer Sheared by an Electroosmotic Flow. We first study the stretching of polymer in the flow direction and its span in the transverse direction of flow. We define the stretching length, L, and the transverse extension, D, as

$$L = \frac{1}{N}\sum_{k=1}^{N}[\max(x_i^k) - \min(x_i^k)] \tag{14}$$

$$D = \frac{1}{N}\sum_{k=1}^{N}[\max(y_i^k) - \min(y_i^k)] \tag{15}$$

where N is the number of time steps for which L and D are computed, x_i^k and y_i^k are the x and y position of polymer bead i at time step k, respectively. Figure 3A shows that L increases continuously as the unscreened electroosmotic velocity u_{eo}° increases, or equivalently, as the external electrical field increases (in all the scaling analysis to follow, we will use u_{eo}° and external electrical field interchangeably as they differs only by a constant for any given surface). Such a trend is expected and is caused by the viscous drag the fluid beads exerted on the polymer chain. Figure 3B shows that D decreases as the external electrical field increases. To understand this, we note that the transverse extension can be modeled as the random walk of blobs in polymer.[11] The blob size, i.e., the local correlation length ξ, depends on the local tension, f, as $\xi = k_BT/f$. Since the local tension varies along the polymer chain, ξ also varies along the polymer chain. However, as done in ref 11, we can approximate the stretched polymer as blobs of uniform size, and $\bar{\xi} = k_BT/(\eta u_{eo}^{\circ})L$, where $\eta u_{eo}^{\circ}L$ is the stokes drag acting on the polymer. Therefore, the transverse extension of the polymer can be estimated to be $D^2 \propto (L/\bar{\xi})\bar{\xi}^2$, i.e., $D^2 \propto k_BT/(\eta u_{eo}^{\circ})$or more specifically $D \propto (u_{eo}^{\circ})^{-1/2}$. While we do not expect a quantitative agreement between the DPD results and blob theory prediction as many assumptions made in the theory are not assumed in the DPD calculation, the trend observed in DPD simulations (Figure 3B) agrees with the blob theory prediction.

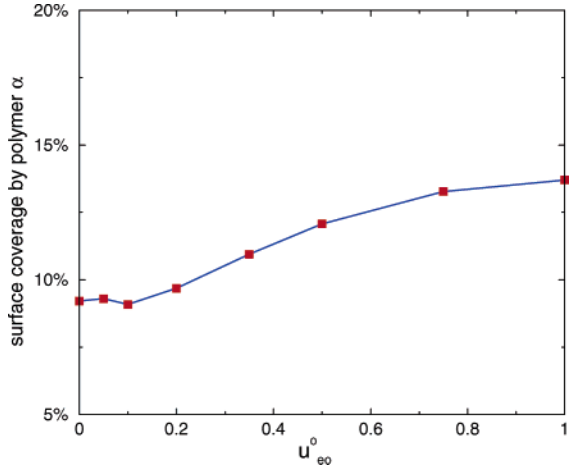

Figure 7. Variation of the coverage ratio of surface by polymers as the unscreened electroosmotic velocity u_{eo}° increases. To compute the coverage ratio, α, we monitor the number of times the channel surface is being hit by fluid beads. α is computed by $\alpha = 1 - N^{hit}/N_{bare}^{hit}$, where N^{hit} and N_{bare}^{hit} are the number of hit per time step by fluid beads when surface is grafted and not grated with polymer, respectively.

To further understand the deformation of polymer chain under the influence of electroosmotic flow, we compute the inclination of polymer θ in the flow direction. The inclination angle is defined as the angle spanned by the unit vector in flow direction and the vector pointing from the anchoring point of a polymer to its center-of-mass. Figure 4A shows that the polymer inclines increasingly as the electroosmotic velocity increases and the inclination angle approaches 12° for the highest electroosmotic velocity studied here. The increased alignment of polymer along the flow direction is consistent with earlier analytical studies and Brownian Dynamics simulations.[31,32] In a sheared flow, the orientation of polymer is determined by the balance between osmotic, shear, and elastic forces of the polymer. Rabin and Alexander considered the competition between these forces in detail, and predicted that $\langle R_e^2\rangle/\langle R_e^2\rangle_o = 1/[1 - \langle\cos\theta\rangle^2]$, where R_e is the end-to-end distance of the polymer chain and the subscript "o" denotes the value in absence of flow. Figure 4B compares the chain stretch and inclination as predicted by the analytical theory,[31] DPD simulations and Brownian Dynamics simulations.[32] We observe that while DPD simulations predict a markedly smaller stretching of polymer at the same inclination compared to the analytical prediction, it follows the same trend. The observed deviation can be attributed to the increased nonlinear elastic restoring force as the polymer is stretched near its full extension. The DPD simulation results are also in good agreement with the Brownian Dynamics simulation results.

The height of polymer coating plays an important role in determining the screening of electroosmotic flow near the surface. The polymer height can be inferred from the polymer density profile. Figure 5A shows the polymer density distribution near the surface at different electroosmotic velocities (external electrical fields). The variation of the density profile near surface is similar to that reported earlier.[23] We observe that as the external electrical field increases, the density peak shifts slightly toward the surface, its value becomes higher and its extension in space becomes narrower, i.e., the polymer become thinner as the external electrical field increases. To examine such thinning more

(31) Rabin, Y.; Alexander, S. *Europhys. Lett.* **1990**, *13*, 49.
(32) Doyle, P. S.; Shaqfeh, E. S. G.; Gast, A. P. *Macromolecules* **1998**, *31*, 5474.

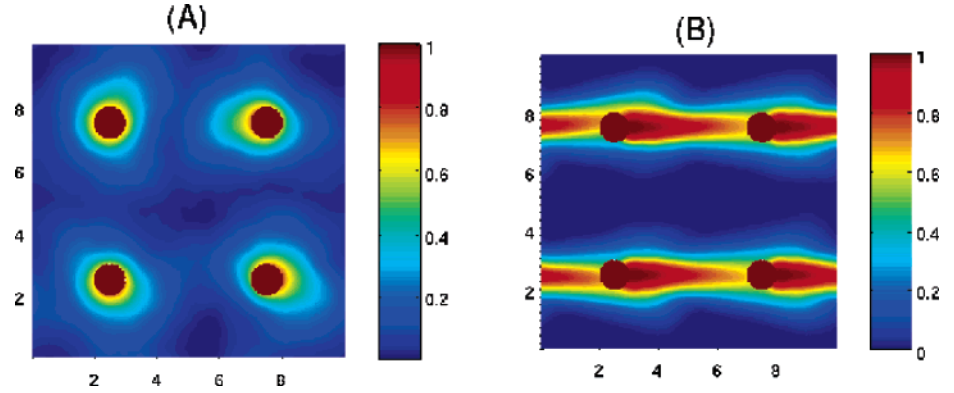

Figure 8. Spatial density distribution of polymer beads in the *xy* plane. The plane is discretized into 1000 × 1000 pixels. At each time step, we project each polymer bead vertically onto the *xy* plane (projection diameter: 1.0) and set the value of surface pixels that are in the shadow of at least one polymer bead to 1.0. For a surface coated homogeneously by polymer, the pixel value will be one uniformly.

quantitatively, we compute an effective polymer height following[23]

$$H_{\text{eff}} = \left(\frac{\int_0^{W/2} \rho_p(z) z^2 \, dz}{\int_0^{W/2} \rho_p(z) \, dz} \right)^{1/2} \tag{16}$$

where $\rho_p(z)$ is the density of polymer bead across the channel and W is the channel height. Figure 5B indicates that while the polymer height decreases slowly at small u_{eo}°, it decreases rapidly as the u_{eo}° increases, and for $u_{eo}^{\circ} = 1.0$, the polymer thickness decreases to 50% of its equilibrium value. Such flow-induced thinning of polymer has been reported in previous Brownian Dynamics and DPD simulations.[23,24,32]

C. Screening of Electroosmotic Flow by Polymer. Figure 6A shows the velocity profiles near the same surface with different unscreened electroosmotic velocities u_{eo}° (achieved by varying the external electrical field). The screening of electroosmotic flow by polymer can be quantified by introducing a screening factor $\beta = 1 - u_c/u_{eo}^{\circ}$, where u_c is the fluid velocity at channel center where the polymer density is zero. Figure 6b shows the scaling of β as a function of u_{eo}°. We observe that in parameter space studied here, the screening of electroosmotic flow decreases nonlinearly as the external electrical field increases.

To understand the above observations, we note that the screening of electroosmotic flow, in the present study where the electrical double layer is assumed to be not affected by the polymer, has two different mechanisms: (1) polymer screens flow by covering the charged channel surface and (2) polymer exerts viscous drag on the fluids.

The coverage of the surface by polymer is affected by the stretching of polymers in the flow direction and the transverse extension and inclination angle of polymers. As the external electrical field increases, the polymers stretch in the flow direction and inclines more closely toward the surface (thus increasing its coverage of the surface). However, at the same time, its transverse extension decreases as shown in Figure 3B and thus tends to lower its coverage of the surface. The net change of the surface coverage by polymer depends on the competition between these different physical processes. Figure 7A shows the variation of the coverage of the surface by the polymer as the external electrical field increases. We observe that the coverage ratio is close to 10% for small external electrical field and increases slightly as the electrical field increases, but overall the coverage ratio is insensitive to the external electric field. The small value of the coverage ratio and its small variation for different external electrical field indicate that the surface coverage by polymer does not play a significant role in determining the flow screening in the present study.

Polymer screens electroosmotic flow also by rendering drag on the fluids. Such an effect is typically modeled by using the Brinkman equation[23]

$$\frac{d^2u}{dz^2} = \frac{u}{k^2} \tag{17}$$

where k is a friction coefficient characterizing the screening characteristics of the polymer layer. For the electroosmotic flow near an open surface with a polymer coating of height H, the velocity boundary conditions are given by $u|_{z=0} = u_{eo}^0$ and $du/dz|_{z=H} = 0$ where u_{eo}^0 is the unscreened electroosmotic velocity. Here it is assumed that the thickness of electrical double layer is thin compared to H. One expects that, in addition to polymer density, the friction coefficient, k, may also depend on other characteristics of the polymer (e.g., alignment in flow direction). However, such dependence is assumed to be much weaker compared the dependence on polymer density. A commonly used model for k is

$$k = \rho_p^{-m} \tag{18}$$

where ρ_p is the local polymer density and m is a positive constant.[23] According to eqs 17 and 18, one expects the local screening of flow become more effective as the local polymer density increases and weaker otherwise. Such a picture only partially agrees with the DPD simulations results.

First, Figure 6A indicates that the flow screening in region $1 \le z \le 4.0$ decreases as u_{eo}^0 increases. For example, u/u_{eo}^0 drops from 0.49 to 0.31 in this region when $u_{eo}^0 = 0.1$, while u/u_{eo}^0 drops from 0.62 to 0.57 in the same region when $u_{eo}^0 = 1.0$. Such a trend is consistent with prediction of eqs 17 and 18, as Figure 5A shows that the local polymer density in this region decreases as u_{eo}^0 increases. Second, Figure 6A indicates that the flow screening in region $z < 1.0$ decreases as u_{eo}^0 increases, i.e., the friction coefficient decreases as u_{eo}^0 increases. This is, however, opposite to the trend predicted by eqs 17 and 18, as Figure 5A shows that the local polymer density in this region increases as u_{eo}^0 increases. We attribute such a discrepancy to the fact that polymers become strongly aligned in the flow direction (and thus the spatial distribution becomes less homogeneous) as u_{eo}^0 increases. Figure 8 shows the spatial density distribution of polymer beads in the *xy* plane for $u_{eo}^{\circ} = 0.0$ and 1.0 for $z < 1.0$. We observe that, as u_{eo}° increases, polymers become strongly aligned in the flow direction. Compared to the globular

conformation, such a polymer conformation is less effective in rendering drag to the fluid. Therefore, despite the increase of local polymer density in region $z < 1.0$, the screening of electroosmotic flow becomes weaker as u_{eo}° increases. In other words, while the friction coefficient, k, depends both on the local polymer density and polymer alignment in the flow direction, we conclude that the dependence on the polymer alignment outweighs the dependence on local polymer density in the parameter space we studied here. Such a strong effect of polymer alignment on flow screening has not been reported in the literature. Such an effect become less significant when the grafting polymer density increases, as the alignment of polymer in flow direction become weaker and the polymers are more homogeneously distributed. Additional simulations indicate that when the number of polymer grafted on channel surface become nine times higher than that in Figure 6, the screening of electroosmotic flow becomes independent of the external electrical field. While the effects reported here might not be important for the screening of pressure-driven flow where a high polymer drafting density is typically used, it is relevant to the screening of electroosmotic flow since even a coarse grafting of polymer is sufficient to significantly lower the electroosmotic flowrate.

IV. Conclusions

By introducing the slip boundary condition, we extended the standard DPD method for the modeling of electroosmotic flow modulation by neutral polymer. The key advantage of the method is that it allows the two-way coupling between polymer deformation and hydrodynamic flow to be modeled in a self-consistent manner. The simulation method was validated by comparing the DPD prediction of flow screening with available analytical solution and by comparing the stretch-inclination characteristics of polymer obtained by using the DPD method and the Brownian Dynamics method. Simulation of the electroosmotic flow screening by dilute polymer coating indicates that, for the parameter space investigated here, the screening of electroosmotic flow become less effective as the external electrical field increases. Detailed analysis of the velocity profiles at different external electrical fields indicated that such a scaling behavior cannot be fully explained by the widely used Brinkman equation if the friction constant in the equation is assumed to depend only on local polymer density. We suggest that the friction constant of polymer layer depends not only on local polymer density but also the alignment of polymer in the flow direction. When the polymer graft density is low, the dependence of the friction coefficient on the polymer alignment can outweigh the dependence on local polymer density. Such an effect should be considered in the design of polymer coating for modulation of electroosmotic flow.

LA063042V